

Coupled Eulerian-Lagrangian (CEL) Modeling of Material Flow in Dissimilar Friction Stir Welding of Aluminum Alloys

M. Safari* and J. Joudaki

Department of Mechanical Engineering, Arak University of Technology, Arak, Iran

ARTICLE INFO

Article history:

Received 23 February 2019

Revised 28 April 2019

Accepted 13 May 2019

Keywords:

Coupled Eulerian-Lagrangian analysis
CEL

Dissimilar friction stir welding

Numerical modeling

Tool pin profile

ABSTRACT

In this work, the finite element simulation of dissimilar friction stir welding process is investigated. The welded materials are AA 6061-T6 and AA 7075-T6 aluminum alloys. For this purpose, a 3D coupled thermo-mechanical finite element model is developed according to the Coupled Eulerian-Lagrangian (CEL) method. The CEL method has the advantages of both Lagrangian and Eulerian approaches, which means it can simultaneously solve the singularity in the large deformation problems and describe the physical boundary of the material accurately. In this paper, the effects of the position of the harder material (AA 7075-T6 aluminum alloy) and the tool pin profile on the temperature distribution and material flow in the weld metal and heat affected zone (HAZ) are investigated. The results show that the material velocity around the FSW tool is found to be higher using a grooved pin profile. Moreover, placing the harder material at the advancing side results in slightly lower process temperatures in comparison to the estimated temperature when the material is placed at the retreating side for all types of tool profiles. It has been proved that if the AA 7075-T6 aluminum alloy is at the advancing side, mixing happens in a thin layer below the tool shoulder, and the penetration of the harder material into the retreating side is found to be limited. In addition, good agreement between the temperature distribution obtained from the experimental measurements and numerical simulations is achieved and the accuracy of the numerical model is confirmed.

© Shiraz University, Shiraz, Iran, 2019

1. Introduction

In recent years, welding of aluminum alloys has been of great interest to researchers due to its strategic applications in industry. For this purpose, various methods have been proposed by researchers for successful welding process of aluminum alloys [1]. Compared with the experimental methods, the numerical simulations are more convenient and effective methods to study the friction stir welding (FSW) process [2]. The main advantages are the visualization of the material flow, temperature field, stresses, and strains' distribution during the whole FSW. Furthermore, the numerical simulation techniques can avoid many repeating experiments and save lots of time and energy. In this way, different modeling techniques, such as

Computational Fluid Dynamics (CFD) and Arbitrary Lagrangian Eulerian (ALE) formulation, were used for the simulation of the FSW process. Seidel et al. [3] developed a 2D thermal model based on the laminar, viscous and non-newtonian flows around a circular cylinder. They observed that significant vertical mixing would occur during the FSW process, especially at low ratios of the welding speed to the rotational speed. Ulysse [4] developed a 3D viscoplastic model to simulate the FSW process using commercial CFD software and studied the effects of the process parameters, including the traverse and rotational speeds, loads on the tool pin, and flow of the particles near the rotating tool. Colegrove and Shercliff [5,6] used a commercial CFD code, FLUENT, to develop a 3D model to determine the temperature distribution and

* Corresponding author

E-mail address: m.safari@arakut.ac.ir (M. Safari)

material flow around a complex threaded tool during the friction stir welding of AA 7075 aluminum alloy. In the model, the no-slip condition was assumed at the tool/workpiece interface and the heat transfer to the backing plate was included in the simulation. Long and Reynolds [7] used a CFD-based model to investigate the effects of the material properties and process parameters on the longitudinal (X-axis) force, material flow, and potential defect formation. Carlone and Palazzo [8] developed a CFD Eulerian model to simulate the FSW process of AA 2024-T3 using the ANSYS CFX software and validated the model by the results of the thermographic observation of the process. By improving the computational power of the computers, the researchers also used Arbitrary Lagrangian Eulerian (ALE) formulation with an explicit solver to simulate the FSW process. Deng and Xu [9] developed a 2D finite element model to simulate the material flow around the FSW tool using Abaqus dynamic explicit solver. The plane strain conditions were assumed in the FE modeling and the experimentally measured temperatures were applied as the body loaded in the model. Schmidt and Hattel [10] developed a thermo-mechanical model to simulate the steady-state FSW of 2xxx aluminum alloy using the coupled temperature-displacement dynamic explicit with the ALE techniques. The results showed that the cooling rate plays a significant role in defect formation, and higher cooling rates lead to the out of order deposition of the materials behind the tool pin. Guerdoux and Fourment [11] developed an adaptive ALE formulation to compute the material flow and temperature distribution. Buffa et al. [12] developed a thermo-mechanical coupled, rigid-visco-plastic, 3D finite element model to investigate the effects of the geometry of the tool on the material flow pattern and the subsequent grain size distribution in the welded joints. The results showed that increase in the pin angle leads to a more uniform temperature distribution along the vertical direction and reduces the distortion of the weld. Assidi and Fourment [13] developed a numerical simulation based on the Forge FE software having considered the ALE formulation and an adaptive remeshing and studied the effect of different friction models on the temperature distribution and material flow. Dialami et al. [14] developed a fully coupled

thermo-mechanical model for FSW simulation. An apropos kinematic setting for different zones of the computational domain was introduced and an efficient coupling strategy was proposed.

Although numerous simulations have been done to characterize the principles of the FSW process, heat generation, material flow and so on, the main challenge in the numerical simulation is to consider the excessive large plastic flow and complex coupling of the thermo-mechanical behaviors in the FSW process. For the CFD technique, the Eulerian mesh is applied. The mesh and the material are independent of each other and there is no mesh distortion problem. However, it is very difficult for the CFD method to capture the material's boundary data and determine the material's boundary accurately. Moreover, in the CFD simulation of the FSW process, the model is incapable of including the effects of the material hardening behavior and elastic properties, and the welding material can be simplified, only, as a rigid viscoplastic material. In addition, when computing the interaction between the welding tool and the workpiece, the full sticking conditions between them are usually assumed, which leads to substantial simulation errors in the estimation of the welding temperature and tool reaction loads. In contrast, the ALE technique can model the boundary conditions as the sliding mode to define the tool-workpiece interaction. The ALE technique can also take into consideration the temperature variation and rate dependency, as well as the material hardening behavior. However, using the Lagrangian elements, some problems arose in the ALE technique. Such elements cannot handle the voids or multiple materials and need to be fully filled with a single material to satisfy the continuity criterion. Therefore, serious mesh distortion will occur in the simulation of large deformation problems such as the FSW process. The mesh distortion of the Lagrangian elements can even cause the model to fail in converge. The Eulerian analysis is based on the volume-of-fluid method where the material is being tracked as it flows through the mesh by computing its Eulerian Volume Fraction (EVF) within each element. Therefore, the Eulerian elements can handle multiple materials as well as void formations, having an advantage over the Lagrangian and ALE [15].

In the current study, a 3D coupled thermo-mechanical finite element model is developed to simulate the FSW process based on the Coupled Eulerian-Lagrangian (CEL) method. The CEL method has the advantages of both the Lagrangian mesh and Eulerian mesh, which means it can solve the element deformation singularity in the large deformation problems and also describe the physical boundary of the material accurately. Therefore, the CEL model has great advantages over the previous numerical models: it can predict the material flow as well as the defect formation during the FSW process explicitly. The main novelty of this paper is that in the simulated model, the convection and radiation heat transfers and the contact heat transfer between the workpiece and the backing plate are all taken into consideration and those parameters have been evaluated by comparing the experimental measurements and numerical simulations. In this paper, first, the simulated model is validated with the experimental measurements. Then, the effects of the harder material position and tool pin profile on the temperature distribution and material flow in the weld metal and Heat Affected Zone (HAZ) are investigated. Due to the high demand for joined dissimilar materials for new structures or parts with mixed material properties, especially in the automotive industry, the AA 6061-T6 and AA 7075-T6 aluminum alloys are selected for the FSW simulation in this study. AA 6061-T6 aluminum alloy has high strength, high corrosion resistance and is made of lightweight aluminum with high ductility and toughness. Meanwhile, AA 7075-T6 exhibits super high strength and has been used extensively in aircraft components and other highly stressed applications. The components of both AA 6061-T6 and AA 7075-T6 aluminum alloys are extensively employed in marine fittings, automobiles and aircraft applications.

2. Numerical Simulation

The FSW process is done at the butt welding position; two sheets are placed near each other. The finite element model is done by the ABAQUS software. Due to the complicated conditions of the FSW process, the model is performed by the coupled temperature-displacement dynamic explicit solver. The sheets are

defined as deformable objects and the tool is rigid. In reality, the sheets are constrained for lateral movement and rotation and the tool moves by a constant speed, but for simulation purposes, the tools are considered to be constant and rotate at the specified rotational speed, and the sheets move toward the tool. A control volume consisting of the sheets is defined and the traverse speed of the tool is defined as the inflow and the outflow over the Eulerian domain boundaries. The tool is the Lagrangian domain boundary.

The frictional condition between the tool and the sheets is very important. The required heat for welding is prepared by the friction between the tool and the sheets. A Coulomb's friction coefficient of 0.7 is defined. Besides, it is assumed that 90% of the inelastic work generated during the process is converted to heat and increases the temperature of the welding zone. The generated heat is transferred into the workpiece and surrounding environment by the conduction, free convection and the radiation mechanism. The temperature distribution affects the mechanical properties of the sheets, softening of the material and better mixing and joining of the welding sheets. The thickness of the sheets is 4mm. The FSW tool has a concave shoulder and a tapered pin made from DIN 1.2344 tool steel (H13) with a threaded line having a 7 mm root diameter, a 3.5 mm tip diameter, and a 7.5 mm height as well as a concave shoulder of 25 mm diameter. To study the effect of the pin profile on the material flow and mixing, three different pin profiles are designed and investigated, namely Smooth, Grooved and Spiral-Grooved pin. Three grooves with a depth of 0.3 mm are created on the lateral side of the pin (Fig. 1), illustrates the FSW tool pins with different profiles in 3D.

The coupled Eulerian-Lagrangian analysis needs defining the regions of the Eulerian solution (the domain of solution) in the model. A space with $50 \times 50 \times 8$ mm³ dimensions is considered as the solution domain. The side dimensions are four times larger than the tool shoulder diameter. The height of the Eulerian domain is 8mm and is larger than its thickness and part of this space will remain empty. This space is held in reserve for unwanted flash formation during the FSW process. A velocity constraint is applied to the Eulerian domain

to prevent the flowing out of the material from the control volume.

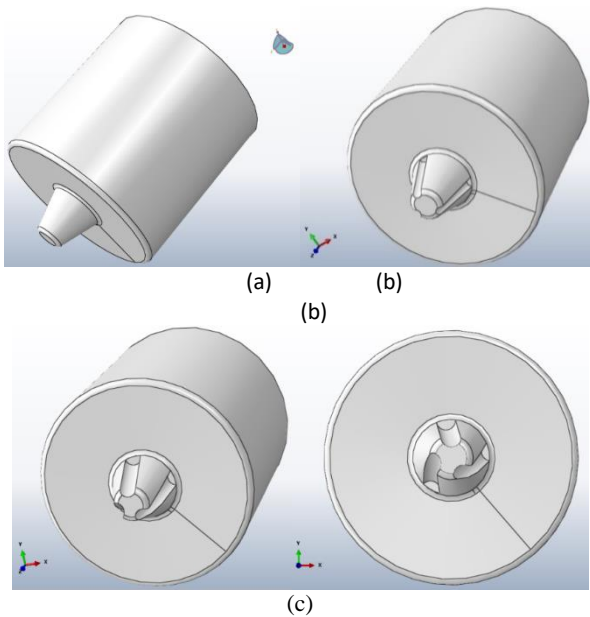


Fig. 1. FSW tool pin profiles; a (Smooth pin) b (Grooved pin), c (Spiral-Grooved pin)

The analysis of the material deformation is complicated and depends on the strain, strain rate and temperature increase. The material model should describe these three influential factors, hence the Johnson-Cook material model is a good choice for describing the plasticity in the CEL analysis. Equation 1 shows the Johnson-Cook plasticity model.

$$\sigma_o = (A + B\bar{\epsilon}_{pl}^n) \left(1 + C \ln \frac{\dot{\epsilon}_{pl}}{\dot{\epsilon}_o}\right) \left(1 - \left(\frac{T - T_{ref}}{T_{melt} - T_{ref}}\right)^m\right) \quad (1)$$

Where σ_o is the flow stress, $\dot{\epsilon}$ is the strain rate, $\bar{\epsilon}_{pl}$ is the effective plastic strain, $\dot{\epsilon}_{pl}$ is the effective plastic strain rate, $\dot{\epsilon}_o$ is the normalizing strain rate (typically 1.0 s^{-1}). T is the temperature (in Kelvin), T_{ref} is the reference temperature (usually room temperature) and T_{melt} is the melting temperature of the material. Here, n is the strain hardening exponent and m is the strain rate sensitivity exponent, and A , B , and C are material constants. The coefficients of the Johnson-Cook plasticity model for AA 7075-T6 and AA 6061-T6 aluminum alloys, used in this analysis, are shown in Table 1.

Table 1. Johnson-Cook plasticity model constants for AA 7075-T6 and AA 6061-T6 aluminum alloys [16, 17]

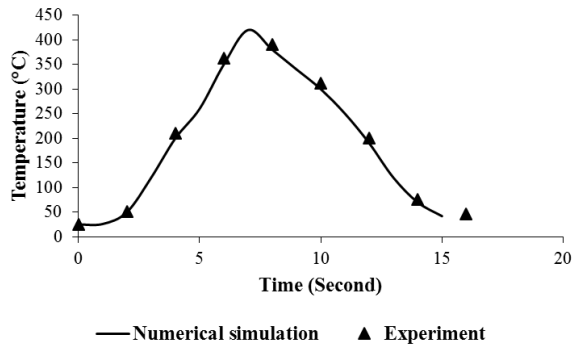
Alloy	A (MPa)	B (MPa)	C	n	m	T_{ref} (°C)	T_{melt} (°C)
AA 7075-T6	546	678	0.024	0.71	1.56	20	635
AA 6061-T6	324	114	0.002	0.42	1.34	20	652

The rigid tool is tilted 2° and constrained in 3D translational movement (axial and radial directions). The tool is meshed by R3D4 rigid elements and the sheets and Eulerian control volume are meshed by EC3D8RT element type. The EC3D8RT element is an 8-node Eulerian continuum element (brick shape) with 4 degrees of freedom at each node (3 displacement DOF and a thermal DOF). The model has been meshed so that a finer mesh exists in the welding zone and the adjacent material deformation zone.

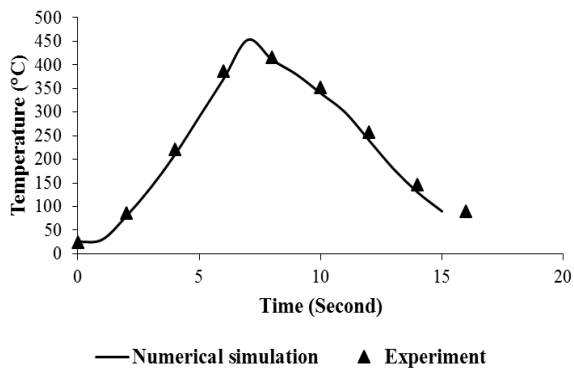
3. Results and Discussion

It is necessary, in the numerical simulation, to evaluate the true heat transfer coefficients in the friction stir welding process. To evaluate the heat transfer coefficients, in the experiments, the temperature is measured using K-type thermocouples at two points with a 10 mm distance from the weld centerline at both advancing and retreating sides. The advancing and retreating sides of the weld line are AA 6061-T6 and AA 7075-T6 aluminum alloys respectively. In the numerical simulations with the same conditions as the experimental work, the temperature profiles at two points, with a 10 mm distance from the weld centerline at both advancing and retreating sides by adjusting the heat transfer coefficients (convection and radiation coefficients and also ambient temperature), are obtained. The extracted temperature profiles from the experiments are compared with those of the finite element simulations to obtain the corresponding heat transfer coefficients. Predicted temperature profiles of the numerical simulations and experimental measurements are shown in Fig. 2. As it is seen in this figure, by adjusting the heat transfer coefficients in the simulation, a good agreement between the experimental and numerical measurements can be obtained. Although there are many parameters that affect the temperature field such as the thermal properties of

the sheet and the heat transfer coefficients, these results indicate that the experimental and numerical temperature fields are in an acceptably close range. The computed convection coefficient, radiation coefficient and ambient temperature from the above-mentioned procedure are 28.3 W/ (m²K), 0.67 and 296.31 K, respectively.



(a)



(b)

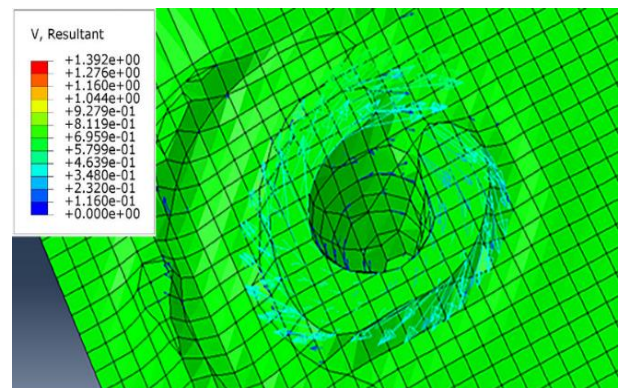
Fig. 2. Temperature profiles of the Grooved pin obtained from the experimental measurement and numerical simulation, a (AA 6061-T6 (advancing side), b (AA 7075-T6 aluminum alloy (retreating side)

The CEL technique is used to investigate the effects of the position of the harder material (AA 7075-T6) relative to the softer material (AA 6061-T6) and of the tool pin profile on the quality of the weld joints prepared by FSW. The following sections will present the results.

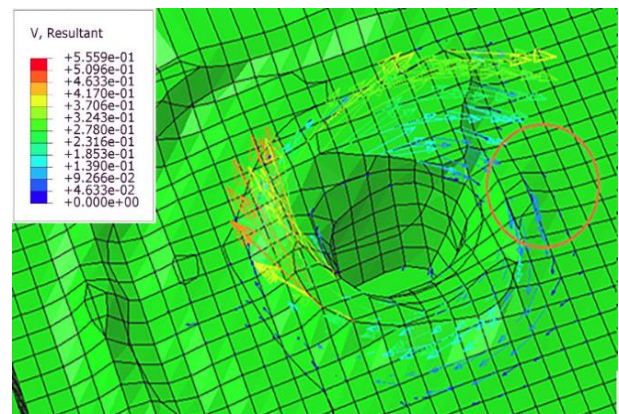
3.1. Effect of pin profile

It is proved that the pin profile can improve the material flow. Better material mixing can be obtained and it leads to higher weld strength [18]. The effect of

the tool pin profiles on the material velocity is shown in Fig. 3. The velocity of the material around the FSW tool obtained from a Eulerian point of view is higher for welds done with a grooved pin. The results of the material velocity show that the material is mixed more uniformly when using the grooved pin. The material flow around the smooth pin is not uniform and the material flow in the specified zone with the red circle is slightly lower than that of the adjacent area. The average material flow velocity is 0.3 and 0.8 m/s around the smooth pin and grooved pin profiles, respectively.



(a)



(b)

Fig. 3. The effect of tool pin profiles on the material velocity; a) Grooved pin, b) Smooth pin.

3.2. Effect of AA 7075-T6 alloy position

When welding dissimilar alloys, the position of the harder material is important and can affect the joint strength. In Fig. 4, the effects of AA 7075-T6 aluminum alloy position on the temperature distribution of a specified point is illustrated for smooth, grooved and grooved-spiral pin profiles. The point is located 10 mm

away from the weld line of the FSW joints. When AA 7075-T6 aluminum alloy (the harder material) is positioned at the advancing side, slightly lower temperatures are obtained for all types of pin profiles. Fig. 5 shows the temperature distribution for different positions of AA 7075-T6 aluminum alloy during the FSW process using a grooved pin. In both situations, the temperature gradient in the softer material (AA 6061-T6 aluminum alloy) is higher than that in the harder material (AA 7075-T6 aluminum alloy). In addition, more symmetry in the temperature distribution (relative to the axis of the tool) is obtained when the harder material (AA 7075-T6 aluminum alloy) is at the advancing side. It is worth mentioning that according to Figs. 4 and 5 the average temperature, in both conditions, is about 450 °C, i.e. below the solidus temperatures of AA 6061-T6 and AA 7075-T6 aluminum alloys. This means that the joint is formed in a solid state. The solidus temperatures for AA 7075-T6 and AA 6061-T6 aluminum alloys are 477 °C and 582 °C, respectively. By placing the harder material (AA 7075-T6 aluminum alloy) at the advancing side, the temperature decreases about 25– 55 °C in comparison to the estimated temperature when the harder material (AA 7075-T6 aluminum alloy) is at the retreating side. Previous researches show that the temperature distribution is dependent on the plastic work, while the plastic work is also affected by the strain rates of the material. The strain rates at the advancing side are much larger than those of the retreating side. When the softer material is placed at the advancing side, the material experiences higher strain rates and consequently higher temperatures [19]. The literature survey diminishes that by placing the softer material (AA 6061-T6 aluminum alloy) at the advancing side, the temperature in some zones can increase to the solid solution temperatures (530 °C) [20, 21] and this causes the dissolution and disappearing of the precipitates in these zones. In addition, the precipitate dissolution could be assisted by severe deformation in the friction stir welding process [22]. Similar results were reported in the FSW of AA 6061-T6 and A356 aluminum alloys by Lee et al. [23].

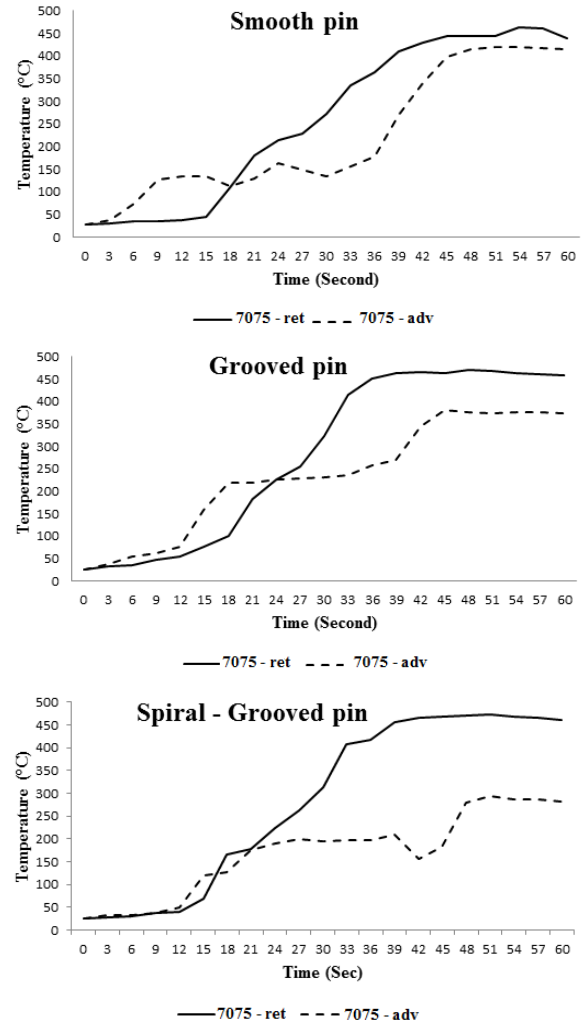


Fig. 4. The effects of AA 7075-T6 position on the temperature profiles for Smooth, Grooved and Grooved-Spiral pin profiles

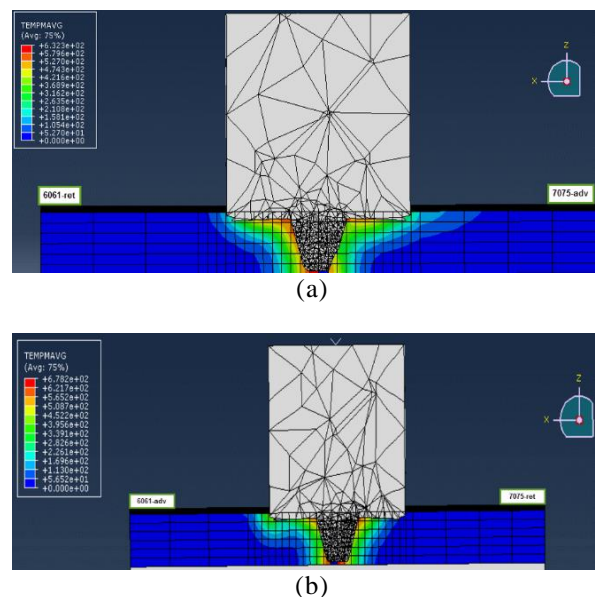


Fig. 5. The temperature distribution during the FSW process for the Grooved pin: a) AA 7075 in the advancing side b) AA 7075 in the retreating side

The material flow within the control volume is computed using the Eulerian Volume Fraction (EVF) option in the ABAQUS software and presented in Fig. 6. Fig. 6 shows the effect of the position of AA 7075-T6 aluminum alloy in the advancing side or retreating side. As it is seen in Fig. 6-a, the mixing of different materials happens in a thin layer below the tool shoulder (in a subsurface layer) when AA 7075 aluminum alloy is located at the advancing side. So, the penetration of the harder material into the retreating side is limited to a thin layer. On the contrary, if AA 6061-T6 aluminum alloy is located at the advancing side (Fig. 6-b), the material mixing happens at a wider zone throughout the sheet thickness, and more material stirring will be obtained. The penetration of the materials in the opposite side can improve the strength of the joint.

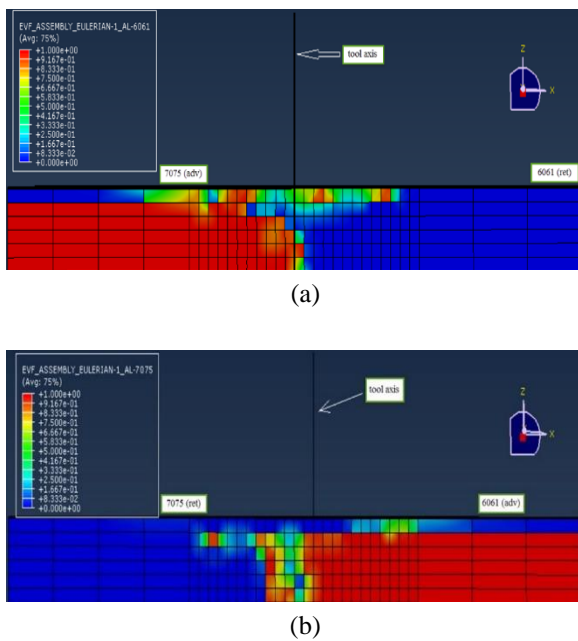


Fig. 6. The material distribution of the Grooved pin across the stir zone using EVF for various conditions; a) AA 7075-T6 located at the advancing side, b) AA 6061-T6 located at the advancing side

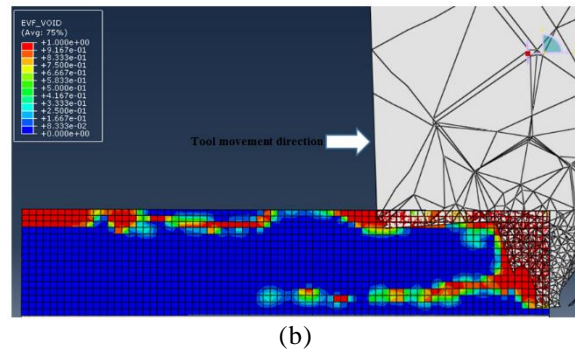
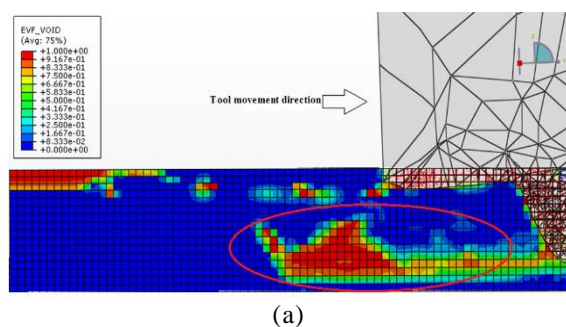


Fig. 7. A comparison of the formation of porosity for Smooth and grooved pin profiles; a) Smooth pin profile, b) Grooved pin profile

4. Conclusion

In this work, the numerical simulation of dissimilar friction stir welding of two common aluminum alloys (AA 6061-T6 and AA 7075-T6) was investigated. For this purpose, a 3D Coupled Eulerian-Lagrangian (CEL) thermo-mechanical FE model was developed in the ABAQUS software. The effects of the harder material (AA 7075-T6) position and pin profile on the temperature distribution and material flow in the welding zone and heat affected zone (HAZ) were investigated. The results of the presented work have been listed below:

1. A good agreement between the temperature distribution extracted from the experimental measurements and numerical simulations was observed. Hence the accuracy of the numerical results was confirmed.
2. The material flow around the FSW tool was higher for welds implemented with the grooved pin and more stirring was obtained.
3. When the harder material (AA 7075-T6) was placed at the advancing side, the temperature distribution was slightly lower than when it was located at the retreating side for all types of tool profiles. Moreover, when using the grooved pin, the estimated temperature distribution in the softer material (AA 6061-T6) was higher than the temperature distribution in the harder material (AA 7075-T6), regardless of AA 7075-T6 position.
4. Using the Eulerian Volume Fraction (EVF) option, it was observed that when the harder material (AA 7075-

T6) was located at advancing side, the material mixing happened in a thin layer below the surface, and the penetration of the harder material into the retreating side was found to be limited. On the other hand, if the softer material (AA 6061-T6) was located at the advancing side, a comprehensively better material mixing was obtained.

5. It was proved that more porosities were created for a smooth type tool due to lack of the stir phenomenon.

5. References

- [1] Faraji, A. H; Moradi, M; Goodarzi, M; Colucci, P; Maletta, C. An investigation on capability of hybrid Nd:YAG laser-TIG welding technology for AA2198 Al-Li alloy, *Optics and Lasers in Engineering*, 96 (2017) 1–6.
- [2] Moradi, M; Ghoreishi, M; Rahmani, A. Numerical and Experimental Study of Geometrical Dimensions on Laser-TIG Hybrid Welding of Stainless Steel 1.4418, *Journal of Modern Processes in Manufacturing and Production*, 5 (2016) 21–31.
- [3] Seidel, T. U; Reynolds, A. P. Two-dimensional friction stir welding process model based on fluid mechanics. *Sci. Technol. Weld. Join.* 8 (2003) 175–183.
- [4] Ulysse, P. Three-dimensional modeling of the friction stir-welding process. *Int. J. Mach. Tools Manuf.* 42 (2002) 1549–1557.
- [5] Colegrove, P. A; Shercliff, H. R. Development of the Trivex friction stir welding tool: Part II-3-Dimensional flow modelling. *Sci. Technol. Weld. Join.* 9 (2004) 352–361.
- [6] Colegrove, P. A; Shercliff, H. R. 3-Dimensional CFD modelling of flow round a threaded friction stir welding tool profile. *J. Mater. Process. Technol.* 169 (2005) 320–327.
- [7] Long, T; Reynolds, A. P. Parametric studies of friction stir welding by commercial fluid dynamics simulation. *Sci. Technol. Weld. Join.* 11 (2013) 200–208.
- [8] Carlone, P; Palazzo, G. S. Influence of process parameters on microstructure and mechanical properties in AA2024-T3 friction stir welding. *Metall. Microstruct. Anal.* 2 (2013) 213–222.
- [9] Deng, X; Xu, S. Two-dimensional finite element simulation of material flow in the friction stir welding process. *J. Manuf. Process.* 6 (2004) 125–133.
- [10] Schmidt, H; Hattel, J. A local model for the thermomechanical conditions in friction stir welding. *Model. Simul. Mater. Sci. Eng.* 13 (2005) 77–93.
- [11] Guerdoux, S; Fourment, L. A 3D numerical simulation of different phases of friction stir welding. *Model. Simul. Mater. Sci. Eng.* 17 (2009) 075001.
- [12] Buffa, G; Hua, J; Shivpuri, R; Fratini, L. Design of the friction stir welding tool using the continuum based FEM model. *Mater. Sci. Eng. A*, 419 (2006) 381–388.
- [13] Assidi, M; Fourment, L. Accurate 3D friction stir welding simulation tool based on friction model calibration. *Int. J. Mater. Form.* 2 (2009) 327–330.
- [14] Dialami, N; Chiumenti, M; Cervera, M; de Saracibar, C. A. An apropos kinematic framework for the numerical modelling of Friction Stir Welding. *Comput. Struct.* 117 (2013) 48–57.
- [15] Al-Badour, F; Merah, N; Shuaib, A; Bazoune, A. Coupled Eulerian Lagrangian finite element modeling of friction stir welding processes. *J. Mater. Process. Technol.* 213(8) (2013) 1433–1439.
- [16] Brar, N.S; Joshi, V.S; Harris, B.W. Constitutive model constants for Al7075-T651 and Al7075-T6, *AIP Conference Proceedings*, Vol, 1195, (2009) 945-948.
- [17] Akram, S; Jaffery, S. H. I; Khan, M; Fahad, M; Mubashar, A; Ali, L. Numerical and experimental investigation of Johnson–Cook material models for aluminum (Al 6061-T6) alloy using orthogonal machining approach. *Adv. Mech. Eng.* 10(9) (2018) 1–14.
- [18] Thimmaraju, P. K; Arakanti, K; Mohan Reddy, G. Ch. Influence of Tool Geometry on Material Flow Pattern in Friction Stir Welding Process. *Int. J. Theor. App. Mech.* 12 (2017) 445–458.
- [19] Jamshidi Aval, H; Serajzadeh, S; Kokabi, A. H. Evolution of microstructures and mechanical properties in similar and dissimilar friction stir welding of AA5086 and AA6061. *Mat. Sci. Eng. A*, 528 (2011) 8071– 8083.
- [20] Shivkumar, S; Ricci, S; Apelian, D. *Production and Electrolysis of Light Metals*, Pergamon, Halifax, (1989) 173–182.

- [21] Shivkumar, S; Ricci, S; Apelian, D. Effect of solution treatment parameters on tensile properties of cast aluminum alloys, *J. Heat Treating*, 8 (1990) 63–70.
- [22] Brett, S; Doherty, R. D. Loss of solute at the fracture surface in fatigued aluminium precipitation-hardened alloys, *Mater. Sci. Eng.*, 32 (1978) 255–265.
- [23] Lee W. B; Yeon Y. M; Jung S. B. The mechanical properties related to the dominant microstructure in the weld zone of dissimilar formed Al alloy joints by friction stir welding. *J Mater Sci*, 38 (2003) 4183– 4191.

مدلسازی کوپل اویلری - لاگرانژی (CEL) جریان ماده در جوشکاری اصطکاکی اغتشاشی غیرمشابه آلیاژهای آلومینیم

مهدی صفری و جلال جودکی

دانشکده مهندسی مکانیک، دانشگاه صنعتی اراک، اراک، ایران.

چکیده

در این پژوهش، شبیه‌سازی اجزای محدود فرآیند جوشکاری اصطکاکی اغتشاشی غیرمشابه بررسی می‌شود. مواد جوش داده شده، آلیاژهای آلومینیوم 6061-T6 و 7075-T6 می‌باشند. بدین منظور، یک مدل اجزای محدود ترمومکانیکال کوپل سه بعدی بر مبنای روش کوپل لاگرانژی - اویلری (CEL) توسعه داده می‌شود. روش CEL مزایای هر دو شبکه‌بندی لاگرانژی و اویلری را دارد و این بدان معناست که این روش نه تنها می‌تواند تغییر شکل المان را در مسائل با تغییر شکل زیاد حل نماید بلکه قادر است که مرز فیزیکی ماده را نیز به طور دقیق ارائه نماید. در این مقاله، اثرات موقعیت ماده مستحکم تر (Al 7075-T6) و پروفیل پین ابزار بر نمودارهای دما و توزیع ماده در فلز جوش و ناحیه متأثر از حرارت بررسی می‌شوند. نتایج نشان می‌دهند که سرعت ماده در اطراف ابزار جوشکاری اصطکاکی اغتشاشی برای ابزار شیاردار بیشتر از سایر ابزارها می‌باشد. همچنین قرارگیری ماده مستحکم تر در سمت پیشروی ابزار منجر به اندکی کاهش دما در مقایسه با قرارگیری ماده مستحکم تر در سمت پسروی ابزار به ازای تمامی پروفیل‌های ابزار می‌شود. ثابت می‌شود که اگر آلومینیم 7075 در سمت پیشروی ابزار قرار بگیرد، اغتشاش در یک لایه نازک زیر شانه ابزار اتفاق می‌افتد و نفوذ ماده مستحکم تر در سمت پسرو محدود می‌شود. به علاوه، یک تطابق خوب بین پروفیل‌های دمای استخراج شده از اندازه‌گیری‌های تجربی و شبیه‌سازی‌های عددی به دست می‌آید و دقت شبیه‌سازی‌های عددی تأیید می‌شود.

واژه‌های کلیدی: آنالیز کوپل اویلری - لاگرانژی، جوشکاری اصطکاکی اغتشاشی غیرمشابه، شبیه‌سازی عددی، پروفیل پین ابزار